ELSEVIER

Journal of Nuclear Materials 266–269 (1999) 376–379

journal of nuclear materials

Spectroscopic measurements of impurity temperatures and parallel ion flows in the DIII-D divertor

R.C. Isler [*,1], N.H. Brooks, W.P. West, A.W. Leonard, G.R. McKee [2], G.D. Porter [3]

General Atomics, 13-357, P.O. Box 85608, San Diego, CA 92186-5608, USA

Abstract

Impurity ion temperatures and parallel flow velocities in the DIII-D divertor have been measured from the shapes and shifts of visible spectral lines of C II, C III, and B II. Spectral multiplet patterns are analyzed by fitting them to theoretical profiles that incorporate exact calculations for the Zeeman/Paschen-Back effect. Both normal flows toward the target plate and reversed flows away from the target plate are observed in the outer divertor leg; only flows toward the plate are detected in the inner leg.

Keywords: Flow; Flow reversal; Doppler broadening; Divertor spectroscopy; DIII-D

1. Introduction

Divertor physics research has constituted one of the major efforts of the DIII-D tokamak program because of the importance of understanding how to manage particle and heat exhausts in power producing fusion devices. The extensive diagnostic array on this machine has made it possible to measure electron temperatures and densities [1] as well as radiative, conductive, and convective power losses [2,3]. Recently, efforts have been initiated both on DIII-D [4,5] and elsewhere [6,7] to measure the flows of impurity and working gas ions which determine convective losses and which have a major influence on the efficiency of the divertor for shielding impurities from the core plasma. Impurity ion temperatures and parallel flow velocities have been examined under a wide variety of conditions; this paper presents some typical results, including the observation of theoretically predicted reverse flow regions.

2. Experimental apparatus and viewing geometry

Spectra in the 4000–9000 Å range are acquired by means of a 1.3 m Czerny–Turner multichordal divertor spectrometer (MDS) equipped with a 1200 l/mm grating. A two-dimensional CCD detector simultaneously records the input signals coming through twelve optical fibers at the entrance slit. The detector integration time is usually set at 125 ms. Fig. 1 (a) and (b) illustrate typical lines-of-sight for this system at two X-point positions. The chords designated V1–V7 are nearly vertical and view the divertor floor through a port near the top of the vacuum vessel. The recently installed tangential views pass through a port near the bottom of the machine and are angled downward. Their projections on a poloidal plane are hyperbolic segments as shown by the curves labeled T2 and T4–T7, which represent five of the ten possible orientations available. Flow velocities along the tangential views are determined from Doppler shifts of emissions with respect to the lineshapes observed in the vertical views, which are essentially perpendicular to the magnetic field. These lines of sight, together with the

* Coressponding author. Tel: +1 619 455 4136; fax: +1 619 455 3569; e-mail: isler@gav.gat.com

[1] Oak Ridge National Laboratory, Oak Ridge, Tennessee, USA.

[2] University of Wisconsin, Madison, Wisconsin, USA.

[3] Lawrence Livermore National Laboratory, California, USA.

0022-3115/99/$ – see front matter
PII: S 0 0 2 2 - 3 1 1 5 (9 8) 0 0 8 2 4 - 1

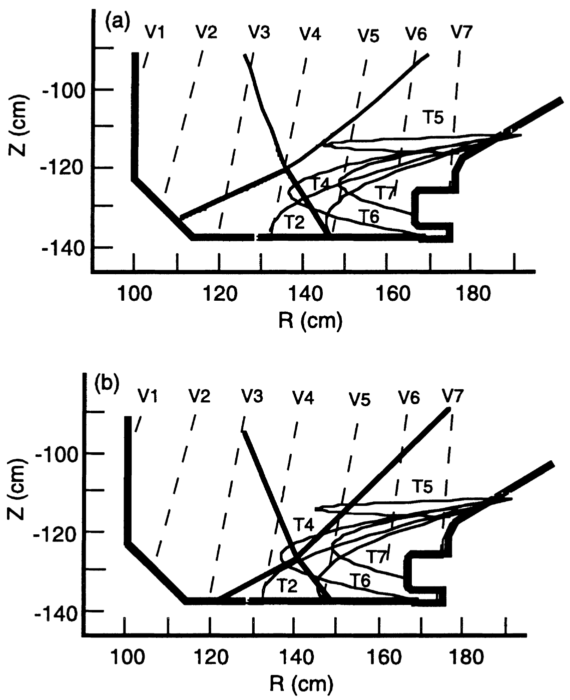

Fig. 1. Vertical views (V1–V7) and tangential views (T2–T7) for obtaining the BII data employed in the present analysis.(a) Separatrix configuration at 3 s, (b) separatrix configuration at 4.4 s.

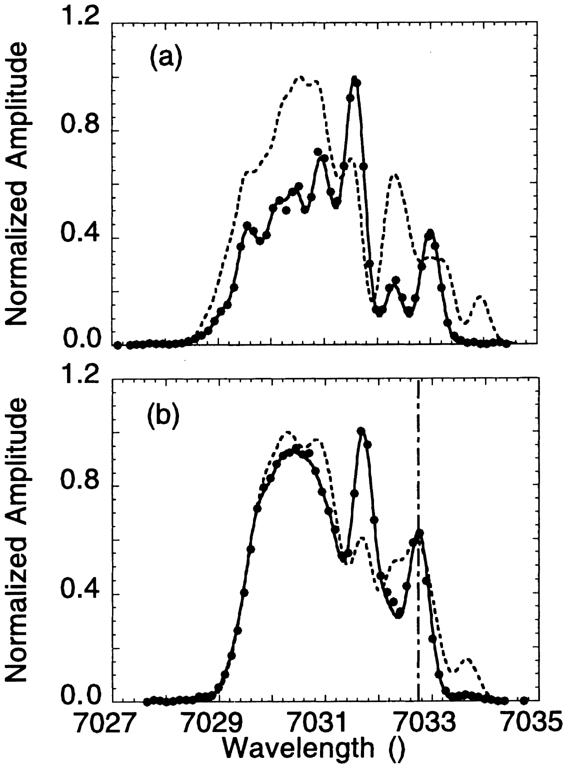

Fig. 2. Profiles of the BII (^{3}P–^{3}S) transition observed along views V2 (a) and V6 (b). Solid circles are measured data; solid lines are the best fit theoretical profiles using the Zeeman/Paschen-Back effect; dotted lines are theoretical profiles if only the low-field linear approximation (Zeeman effect) is employed.

ability to sweep the X-point radially, allow spectroscopic sampling of most of the divertor plasma.

3. Ion temperatures

Most of the analyses of the ion characteristics have utilized the B II triplet (^{3}P–^{3}S) around 7335 Å, the C II doublet (^{2}P–^{2}S) near 6579 Å, and the C III triplet (^{3}P–^{3}S) near 4649 Å. Only temperatures determined from the vertical views are discussed in this section. These are believed to be more accurate than those deduced from the signals coming through the tangential views. This point will be discussed further in Section 4.

Because ion temperatures in the divertor are usually less than 20 eV, it is necessary to account accurately for the nonlinear splitting of the sublevels of excited electronic states in a magnetic field (Zeeman/Paschen-Back effect) when determining the Doppler widths [3,8]. Of all the transitions utilized for temperature measurements, deviations from a linear dependence on the field (Zeeman effect) appear most markedly in the B II multiplet, although they are also evident in the other multiplets. Typical measurements from views V2 and V6 are shown by the solid circles in Fig. 2. In the absence of a magnetic field, this multiplet would appear as three closely spaced spectral lines, but the observed patterns are much more complicated and are qualitatively disparate in the two views because of the difference in field strength as a function of major radius. In order to obtain the maximum count rate, polarizers are not used in the optical path, therefore, the sum of the amplitudes of the σ- and π-components are equal. Ion temperatures are determined from the theoretical lineshapes that give the best fit to the entire multiplet for a given field strength. Since the spectroscopic signals are integrated over the entire sightline, it is not a priori evident that they will reflect a single temperature. However, both sets of data in Fig. 2 are well represented by profiles computed for a single ion temperature as shown by the solid curves. Low-field linear approximations of the theoretical profiles are shown as dashed curves to emphasize the necessity of including nonlinear effects into the analysis.

The discharges producing the data of Fig. 2 are operated at 2.01 T and 1.36 MA. At 1.5 s a strong gas puff raises the density, and the neutral-beam injection power is increased from 2.2 to 5 MW. The inner leg of the divertor is detached while the outer remains attached throughout the discharge.

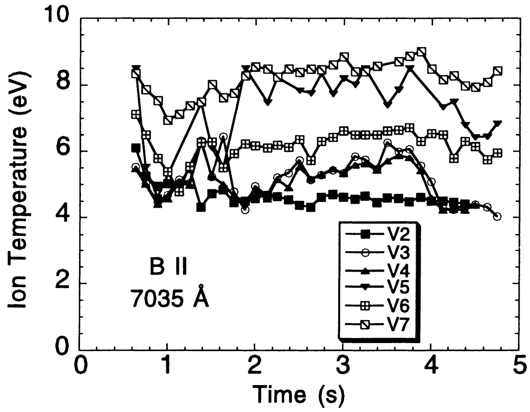

Fig. 3. Time histories of BII temperatures measured along the vertical views.

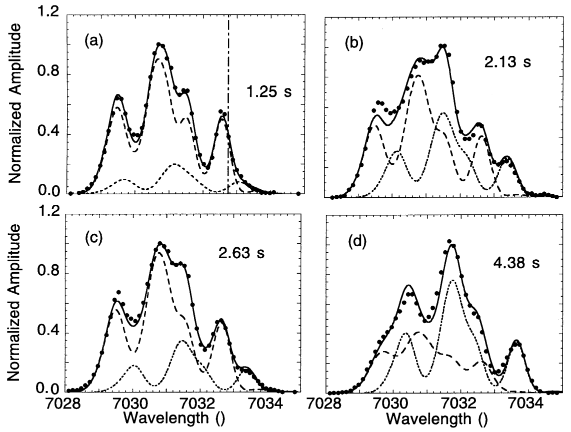

Fig. 4. Line shapes of the BII doublet at 7035 Å observed along view T2 at four times. Solid points are measured data. The net theoretical curve (solid) is composed of a blue-shifted (dashed) and red-shifted (dotted) components.

B II temperatures as a function of time are shown in Fig. 3. From about 1.8–3.4 s no further major changes are made in operating conditions. The highest temperatures, around 8 eV, are recorded from V5 which intercepts the outer strike point and from V7 which most likely detects its strongest signals upstream of the divertor region. Temperatures observed from the inner leg are in the 4–5 eV range. For strong signals, such as those shown in Fig. 2, the uncertainty in ion temperature appears to be 1 eV or less, which is evident in the the small scatter of the data points during the quasi-steady segment of the discharge. After 3.4 s the X-point is swept outward in major radius. By 4.4 s V3 and V4 pass through the inner, rather than the outer leg (Fig. 1(b)), and the observed temperatures are the same as that along V2.

4. Flow velocities

Signals from view T2 at four different times are shown in Fig. 4. The σ-components strongly dominate these lineshapes so they do not resemble those from the vertical views. In general, the data points cannot be fitted by a single multiplet profile, but they can usually be fitted by two profiles with different Doppler shifts as shown by the dashed and dotted lines. The solid lines are the sum of the two profiles. Although the theoretical fits are not perfect, they are close enough to the measured data to confirm that the major contributions to the signals come from two distinct groups of ions.

A qualitative indication of the shifts can be obtained from the fact that calculations show the peak at 7032.75 Å should appear at the same wavelength in views V6 and T2 if there is no parallel flow. The dot-dash vertical marker in Fig. 2(b) is located to pass through this local maximum. In Fig. 4(a) it is seen that this peak in the stronger component (dashed line) is blue-shifted with respect to the marker; in the DIII-D geometry a blue shift indicates that the radiating ions are moving toward the target plate. However, the weaker component is red-shifted and is indicative of a group of ions flowing in the reversed direction. This behavior, which is theoretically predicted to occur under certain circumstances [9], is generally observed in C II, C III, and B II during most types of discharge conditions. Specific modelling of C II behavior in attached DIII-D plasmas using the UEDGE code [10] do indeed indicate two intensity maxima near the locations inferred from experiment. The modelled velocity patterns are quite complex, but they show reversal near the separatrix while indicating normal flows are present at larger radii.

Reversed-flow components are even more obvious in Fig. 4(b) and (c) after the gas is added and the neutral beam injection power is increased. By 4.38 s the change of the magnetic configuration has positioned view T2 closer to the X-point [see Fig. 1(b)] where the intensity is stronger and the reversed component dominates the signal. Although the emitting ions may be distributed over several centimeters of the sightline, the variation of the multiplet patterns as a function of magnetic field strength makes it possible to determine the approximate radial locations of the most intense regions. For chords that cross the same radial location twice, the vertical position is ambiguous without supplementary data. The estimated error of the origin of signals shown in Fig. 4 is ±5 cm, although the radiators often appear to be well enough localized that the position of the most intense group can be ascertained within ±3 cm. The position of the weaker group may be less certain depending on signal strength.

Table 1
Flow velocities, Mach numbers, and average positions for normal- and reversed-flow B II ions

Time (s)	Normal-flow ions			Reversed-flow ions		
	Velocity (10^6 cm/s)	Mach No.	Radius (m)	Velocity (10^6 cm/s)	Mach No.	Radius (m)
1.25	1.02	0.48	1.58	−0.51	0.24	1.34
2.13	0.75	0.35	1.58	−2.52	1.17	1.44
2.63	0.69	0.32	1.64	−2.09	0.98	1.49
4.38	1.27	0.59	1.64	−3.58	1.66	1.42

Table 1 shows velocities, Mach numbers, and most probable positions in major radius of the B II ions observed at the four times indicated in Fig. 4. The Mach numbers are computed with respect to the deuterium sound velocities by assuming an average temperature of 7 eV which corresponds to the B II ion temperatures in the outer leg as obtained from the vertical views. Ion temperatures interpreted from the tangential views are generally 2–4 eV greater than those from the vertical views. It is believed that this difference is an artifact caused by variations in the flow speed along the tangential lines-of-sight and by differences in the excited state sublevel splitting owing to the radial variation of the magnetic field. The possibility that the differences may be real cannot be completely ruled out, however. For most of the cases that have been analyzed, the normal-flow Mach numbers range from 0.3–0.7, whereas the reversed-flow values are near Mach 1. By referring to Fig. 1, it can be seen that the normal-flow group is interpreted to be at major radii 15–20 cm to the low-field side of the separatrix. This conclusion is substantiated by the fact that intensities from the vertical views are by far the strongest along V6 which intercepts the target plate at a major radius of 162 cm (Fig. 1) in good agreement with the inferred radii of 1.58–1.64 m listed in Table 1. The best fits to the data indicate that the reversed-flow group lies within a few cm of the separatrix.

If the X-point is moved very far outward, the inner leg overlaps some of the tangential views. In many cases the radiation from a particular ion is much stronger in the inner leg than it is in the outer, and the normal-flow signals are red-shifted. In these cases inner leg flows can be distinguished, and the minor contribution to the red-shifted emission pattern from the reversed-flow ions on the outside does not significantly affect their velocity measurements. The magnitudes of these normal flow velocities tend to be comparable to those observed for the reversed group in the outer leg, i.e., near Mach 1.

5. Summary

Ion temperatures for B II, C II, and C III have been measured under a variety of conditions in the DIII-D divertor and are usually in the range of 4–20 eV. Velocities determined from Doppler shifts indicate that normal flows in the outer leg vary from 3×10^5 – 1.5×10^6 cm/s (Mach 0.3–0.7) whereas on the inner leg they are 1×10^6 – 3.5×10^6 cm/s (generally near Mach 1). Reversed flow regions exist in the outer leg during most types of operation, and the magnitude of their velocities tends to correspond to those of the normal flows on the inner leg.

Acknowledgements

This work was performed for the US Department of Energy under contract numbers DE-AC05-96OR22464 with Oak Ridge National Laboratory, managed by Lockheed Martin Energy Research Corp., DE-AC03-89ER51114 with General Atomics, and W-7405-ENG-48 with Lawerence Livermore National Laboratory

References

[1] T.N. Carlstrom, C.L. Hsieh, R.E. Stockdale, D.G. Nilson, D.N. Hill, Rev. Sci. Instrum. 68 (1997) 1195.
[2] A.W. Leonard, M.A. Mahdavi, S.L. Allen, N.H. Brooks, M.E. Fenstermacher, D.N. Hill, C.J. Lasnier, R. Maingi, G.D. Porter, T.W. Petrie, J.G. Watkins, W.P. West, Phys. Rev. Lett. 78 (1997) 4769.
[3] R.C. Isler, R.D. Wood, C.C. Klepper, N.H. Brooks, M.E. Fenstermacher, A.W. Leonard, Phys. Plasmas 4 (1997) 355.
[4] R.C. Isler, N.H. Brooks, W.P. West, A.W. Leonard, and G. R. McKee, Normal and Reversed Impurity Flows in the DIII-D Divertor, General Atomics Report GA-A22815, 1998.
[5] J.A. Boedo, R. Lehmer, R.A. Moyer, J.G. Watkins, and N. Wolf, these Proceedings.
[6] J. Gafert, K. Behringer, D. Coster, C. Dom, K. Hirsch, M. Niethammer, U. Schumacher, the ASDEX Upgrade team, Plasma Phys. Control. Fusion 39 (1997) 1981.
[7] B. LaBombard et al., J. Nucl. Mater. 241–243 (1997) 149.
[8] J.D. Hey, Y.Y. Lie, D. Rusbüldt, E. Hintz, submitted to Plasma Phys. 34 (1994) 725.
[9] P.C. Stangeby, J.D. Elder, D. Reiter, G.P. Maddison, Contrib. Plasma Phys. 34 (1994) 306.
[10] T. Rognlien, J.L. Milovich, M.E. Resnik, G.D. Porter, J. Nucl. Mater 196–198 (1992) 347.